

## Energy Analysis During the Collision of Two Successive CMEs

Fang Shen,<sup>1</sup> Chenglong Shen,<sup>2</sup> Yuming Wang,<sup>2</sup> Xueshang Feng,<sup>1</sup> and Changqing Xiang<sup>1</sup>

<sup>1</sup>*SIGMA Weather Group, State Key Laboratory of Space Weather, Center for Space Science and Applied Research, Chinese Academy of Sciences, Beijing 100190, China*

<sup>2</sup>*School of Earth and Space Sciences, University of Science and Technology of China, Hefei, Anhui 230026, China*

**Abstract.** Three-dimensional (3D) numerical magnetohydrodynamic (MHD) simulation is carried out for the two successive slow CMEs with initial speeds of 240 km/s and 410 km/s, in order to study a scenario of the collision process of these two CMEs. Based on the 3D numerical results, the energies including the kinetic, magnetic, internal and gravitational potential energy are studied in detail. Energy analysis during the propagation and interaction of the two CMEs show that we are able to in principle reproduce the super-elastic collision process for this scenario which supports the conclusions made by C. Shen et al. (2012) (hereinafter referred to as paper 1) for a comprehensive picture of a unique collision between two CMEs for the 2 November 2008 event observed by STEREO Spacecraft in the heliosphere.

### 1. Introduction

Previous work has shown that successive ICMEs can merge with each other and form a compound structure by the help of the coronagraphic observations and the presence of the solar wind measurement in the outer heliosphere, as mentioned formerly (Burlaga et al. 2002; Lugaz and Roussev 2011). The coronal mass ejections (CMEs) interaction and their complex structures have been widely reported and studied based on observations and MHD simulations (Burlaga et al. 2002; Wang et al. 2003; Lugaz et al. 2005; Lugaz and Roussev 2011; Shen et al. 2011, 2012). Previous results show that the complex structure formed from the interaction between multiple CMEs are thought to be the major cause of the great geomagnetic storm (Wang et al. 2003; Lugaz et al. 2005). There are several topics related to CMEs interaction that require further investigation, such as the momentum exchange between the successive eruptions during their interaction, the fate of the related shocks, and the deflection and rotation of the CME during the interaction. Especially, the energy analysis has not been studied in the previous numerical simulation for the CMEs interaction.

A superelastic collision is an unusual process in which some mechanism causes the kinetic energy of the system to increase (paper 1). Recently, C. Shen et al. (2012) present a comprehensive picture of a unique collision between two CMEs in the heliosphere, which are the two magnetized plasmoids erupting from the Sun. And their analysis show that these two magnetized plasmoids collided as if they were solid-like

objects, with a likelihood of 73% that the collision was superelastic. The total kinetic energy of the plasmoid system increased about 6.6% through the collision for the 2 November 2008 event. But it remains unclear what is the source of the net kinetic energy gain and how does the energy convert, which are the key factors for superelastic collisions. In this paper, we will present an energy analysis based on our work (Shen et al. 2011, 2012) for two successive CMEs similar to the CMEs on 2 November 2008 to examine the energy evolution and conversion during the two CMEs propagation and interaction, in order to verify the superelastic collision process and to reveal the energy conversion. Similar to our previous study (Shen et al. 2011, 2012), these two CMEs are mimicked by two opposite polarity plasma blobs, where the magnetic topology exclude reconnection.

In this paper, we carry out three-dimensional (3-D) MHD simulations based on the observations of the 2008 November event and try to reveal the nature of the CMEs' collision through the analysis of the energy transformation during the collision. In the next section, the MHD model and simulation method are introduced. The simulation results of the CMEs' collision is presented in sections 3. In the last section, a comparison with a non-collision case and a discussion are given.

## 2. MHD Model and Simulation Method

We have constructed a 3D COIN-TVD (Corona-interplanetary total variation diminishing) MHD model in our previous study to investigate the evolution and interaction of two successive CMEs in the ambient solar wind (Shen et al. 2011, 2012). The background solar wind is constructed based on the observed line-of-sight of magnetic field from 1 Rs to the Earth's orbit (215 Rs) and beyond. In our COIN-TVD MHD model, a modified Total Variation Diminishing /Lax-Friedrichs (TVD/LF) type scheme (Shen et al. 2011) is applied as the numerical 3D MHD scheme with the observed line-of-sight of magnetic field by WSO as initial input and with the projected characteristic boundary conditions as the lower boundary condition. The computational domain here covers  $1 \text{ Rs} \leq r \leq 100 \text{ Rs}$ ;  $-89^\circ \leq \theta \leq 89^\circ$  and  $0^\circ \leq \phi \leq 360^\circ$ . The detailed description about the the grid mesh, the asynchronous and parallel time-marching method and the initial-boundary conditions for this 3D MHD simulation are given in Shen et al. (2011, 2012) and omitted here.

Our scenario is motivated by the two successive CMEs occurring on 2008 November 2 studied in paper 1. In configuring this scenario, these two CMEs are simulated by means of two high-density, -velocity and -temperature magnetized plasma blobs model, and successively ejected into the nonhomogeneous background solar wind medium along different initial launch directions, respectively (Shen et al. 2011, 2012). In our simulation, the radius of each plasma blob  $a_{cme}$  is set as 0.5 Rs. The centers of the initial plasma blobs are situated at (2.0 Rs, N6W28) and (2.0 Rs, N16W08), respectively, whose directions are identical to that in paper 1. The second plasma blob is initiated 6 hrs after the launch of the first one. The maximum velocities of the plasma blobs center are set as  $3 \times 243 \text{ km/s}$  and  $3 \times 407 \text{ km/s}$  to make the average velocities of the two plasma blobs consistent with the CME velocities deduced from the observation data in paper 1, by assuming the average velocity of the plasma blob approximately equal to 1/3 of the maximum velocity inside the blob (Shen et al. 2011). The initial energy inputs of two simulated CMEs and the energy of the background solar wind are given in Table 1.

Table 1. Energy Inputs of CME1, CME2 and Background Solar Wind energy

	CME1	CME2	Solar Wind
Kinetic Energy ( $E_k, \times 10^{32}$ erg)	0.077	0.261	5.30
Magnetic Energy ( $E_m, \times 10^{32}$ erg)	0.104	0.15	3.11
Internal Energy ( $E_i, \times 10^{32}$ erg)	0.097	0.145	7.28
Gravitational Energy ( $E_g, \times 10^{32}$ erg)	-0.064	-0.088	-2.52
Total Energy ( $E_t, \times 10^{32}$ erg)	0.213	0.468	13.2

### 3. Simulation Results

To identify the two CMEs, we use the value of the radial velocity being  $>450$  km/s as the criterion to identify the position of the CME. Figure 1 shows the 3D propagation of the simulated CMEs at 7 hours (a), 10 hours (b) and 15 hours (c) after CME1's launch, respectively. The magnitude of the radial velocity and the magnetic field topology in Figure 1 are represented by the color code and the rod-shaped magenta lines, respectively.

Since CME2 is faster than CME1, the two CMEs get closer and closer as shown in the three panels. The momentum transfer could be clearly seen by noting the orange region. At 7 hours, right before the collision, the orange region, which denotes a radial velocity of 600 km/s, locates in CME2. After the two CMEs touch, the orange region moves forward, which suggests a momentum transfer from CME2 to CME1.

With some limits of the MHD code, however, we cannot identify the exact boundary of a CME. Thus, we do not analyze the momentum or energy change for individual CMEs, but instead, analyze the variations of all kinds of energies integrated over the whole computational domain. All the energies of the two CMEs and solar wind at initial time are shown in Table 1. Although the energy of the two CMEs is only about 5% of the total energy of background solar wind, it is larger than the errors unavoidably from numerical calculations and ideal MHD assumptions as will be seen below.

The solid black line in the top panel of Figure 3 shows the variation of the total energy,  $E_{tot}$ , an integrated value over the whole computational domain, after the launch of CME2 at  $t = 6$  hours. The quick drop of  $E_{tot}$  at the beginning is because the introduced CME expels the ambient solar wind. This is a numerical effect and brings difficulty into the analysis of energy variation. To reduce it, we first calculate the net energy flowing into the computational domain at boundaries in a time interval  $\Delta t$ , which is  $E_b = \Delta t \int \varepsilon_t \rho \mathbf{v} \cdot d\mathbf{S}$  where  $\varepsilon_t$  is the energy density at time  $t$  and  $\mathbf{S}$  is the surface of the boundaries, and then deduct it from the total energy to get a corrected energy. Assume that the total energy at any given instant  $t_i$  is  $E_{ti}$  and the net energy flow across the boundaries since the last instant  $t_{i-1}$  is  $E_{bi}$ , the correct total energy is  $E_{tot} = E_{ti} - \sum_1^i E_{bi}$ , which should be always equal to the total energy at initial time  $t_0$  in theory. After the correction, the total energy varies in small range of about  $5 \times 10^{29}$  erg as shown by the solid blue line in the top panel of Figure 2 that just indicates the numerical error in our simulation. It is much smaller than the CME energies listed in TABLE 1.

All kinds of energies after the correction are shown in the other panels in Figure 3. After the two CMEs propagate into the computational domain, the kinetic energy,  $E_K$ , and gravitational energy,  $E_G$ , both continuously increase, whereas the magnetic energy,  $E_B$ , and thermal energy,  $E_t$ , both decrease. The changes of these energies are all one

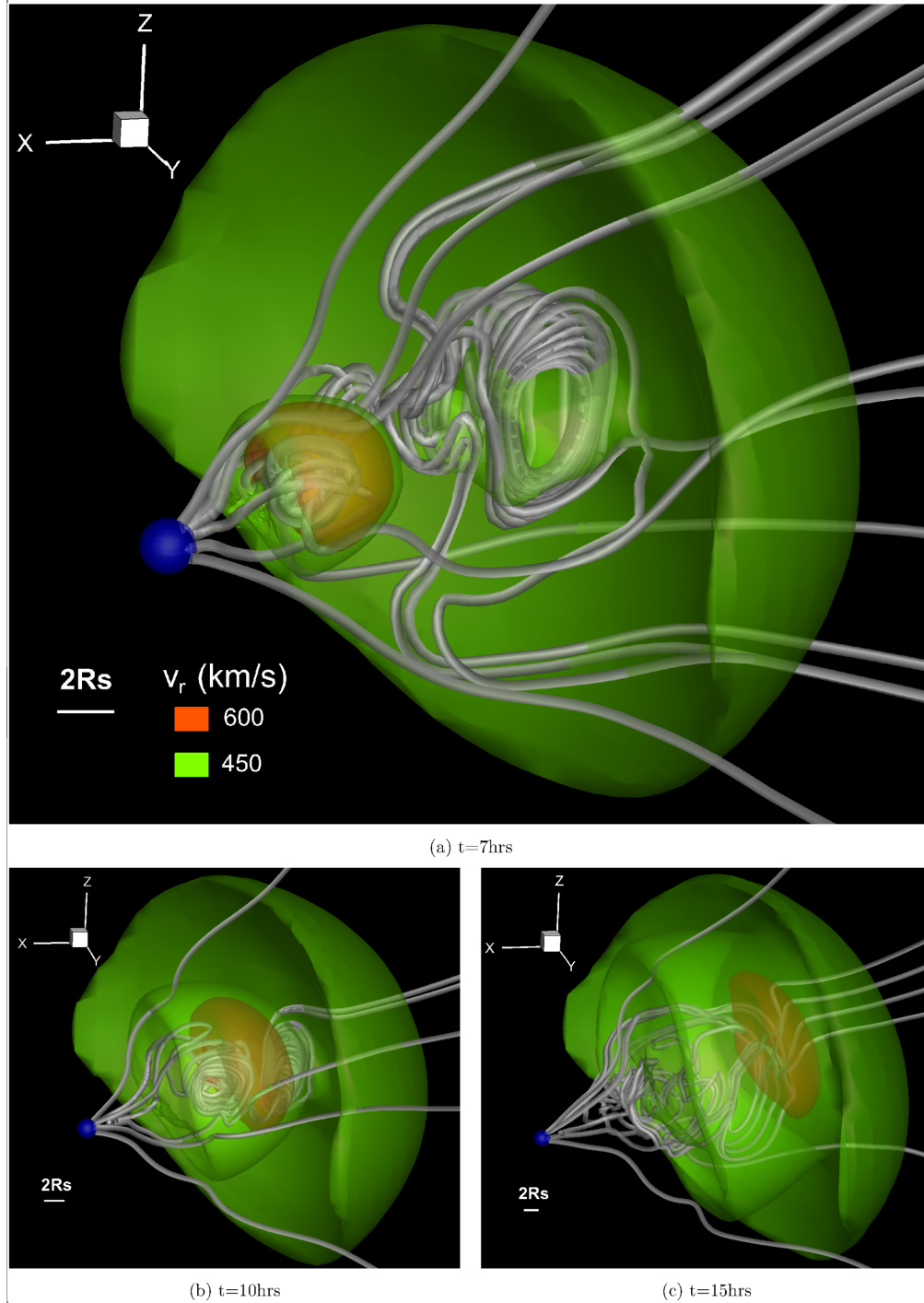


Figure 1. Radial velocity map of the two CMEs at the time of 7, 10, and 15 hours. The surfaces of the radial velocity being 450 and 600 km s<sup>-1</sup> are displayed by different colors. Some magnetic field lines are shown as the thick white lines. The small blue ball shows the position and size of the Sun.

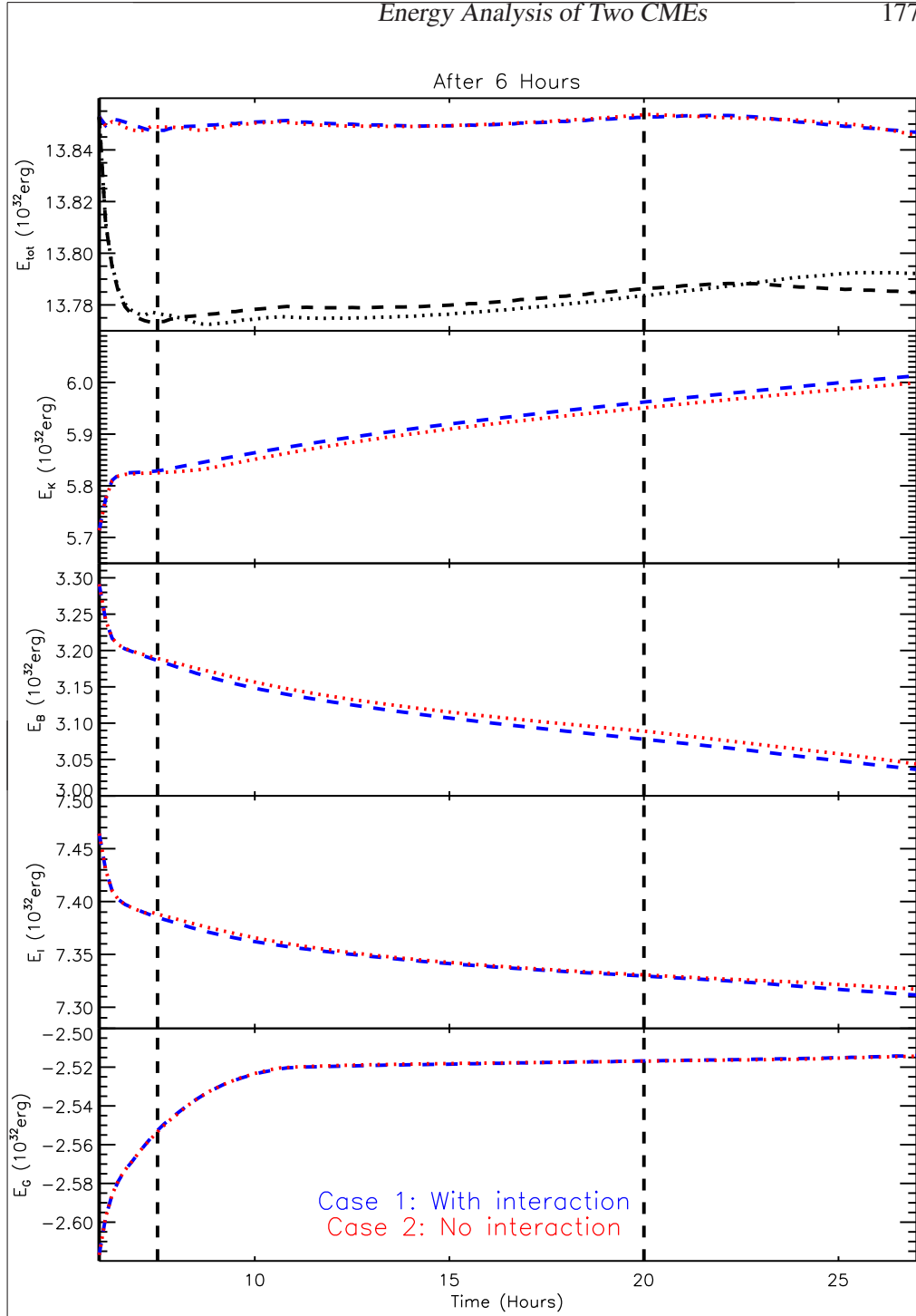


Figure 2. Temporal profiles of all kinds of energies. The panels from the top to the bottom show the total energy  $E_{tot}$ , kinetic energy  $E_K$ , magnetic energy  $E_B$ , thermal energy  $E_T$ , and gravitational energy  $E_G$ , respectively. The vertical dashed lines mark the beginning and the possible ending time of the collision. In the top panel, the black lines shows the total energy before correction (see main text for details).

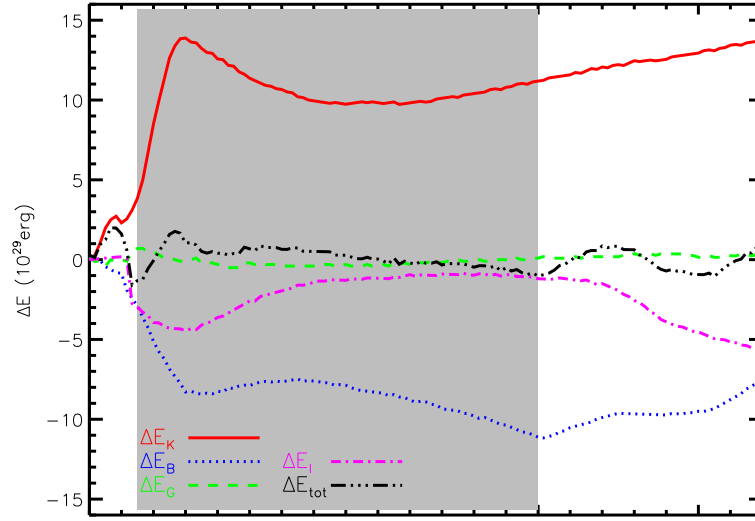


Figure 3. Energy difference between the case of collision (Case 1) and the case of non-collision (Case 2). A positive value means that the energy in Case 1 is larger than that in Case 2. The shadow area mark the beginning and the possible ending time of the collision.

order larger than the variation of total energy, suggesting a real physical process. The increase of  $E_G$  is due to the CMEs carrying heavier plasma than the background solar wind. The changes of other energies are consistent with the well known picture that the CME's magnetic and thermal energy will be converted into kinetic energy as it expands during the propagation (Wang et al. 2009).

In order to validate that the kinetic energy gain (or partial of it) comes from a superelastic collision, we need another case for comparison, in which the two CMEs do not collide. To do this, we adjust the longitude of CME2 to  $165^\circ$ , which causes the longitudinal separation between the two CMEs to be  $175^\circ$  and keep all the other parameters exactly the same as those in the case of collision. Hereafter we use Case 1 for collision, Case 2 for non-collision and CME2' for the second CME in Case 2.

#### 4. Comparison and Discussion

From CME1 being introduced into computational domain to the instance of CME2 being introduced, the two cases are exactly the same. After CME2 is introduced, the two cases become different. The dashed blue lines in Figure 3 show the energy variations for Case 2, which are similar to those in Case 1 except some small differences. These small differences are shown much clearly in Figure 3.

The difference of the total energy,  $\Delta E_{tot}$ , between the two cases has small fluctuations with an amplitude of about  $2 \times 10^{29}$  erg. It indicates the level of numerical error. The difference of the gravitational energy,  $\Delta E_G$ , is about  $10^{29}$  erg, smaller than the numerical error. Thus, we cannot conclude if  $\Delta E_G$  is real or not. For all the other energies, the differences are significantly larger than the error and thought to be physically meaningful.



It is found that from the time of  $t = 7$  hours, the difference of the kinetic energy,  $\Delta E_k$ , rapidly increases from about  $2 \times 10^{29}$  erg to about  $1.4 \times 10^{30}$  erg in 2 hours, and then decreases back to about  $10^{30}$  erg and slowly returns. It means that there is extra kinetic energy gain in Case 1. And the extra kinetic energy gain must come from the collision of the two CMEs. Although we do not know the kinetic energy for each CME, the comparison between Case 2 and Case 1 is just like the comparison between the state before and after the collision. The significant difference between the two cases in the kinetic energy does confirm that the collision of CMEs could be superelastic as suggested by C. Shen et al. (2012).

It is hard to identify when the collision ends. It might be at  $t = 20$  hours or even later. But we are sure that the two CMEs have fully interacted for a long time. This long process allows magnetic and thermal energies to be converted into kinetic energy. It is noticed that the decrease of the magnetic energy is much larger than that of the thermal energy, which suggests that the magnetic energy stored in CMEs is the major source of the extra kinetic energy gain.

In this study, the initial kinetic energy of the two CMEs is about  $33.8 \times 10^{30}$  erg (see TABLE 1). Since the collision happens quickly after the introductions of the CMEs, we may use this value approximately as the CMEs' kinetic energy right before the collision. The extra kinetic energy gain due to the collision is on the order of  $10^{30}$  erg. It is therefore derived that the superelastic collision of the two CMEs causes their total kinetic energy increased by about 3C4%, which is close to the value of 6.6% given by C. Shen et al. (2012). Assuming the energy gain totally goes to CME1, we then estimate that the kinetic energy of CME1 increases by about 13%.

In this paper, we only consider the CMEs similar to the 2008 November event. It is not clear if the collision between any CMEs is superelastic. Moreover, some open questions remain. For example, how are the magnetic or thermal energies convert into kinetic energy? How does magnetic reconnection influence the collision process and result if it efficiently occurred? All these questions are worthy of further studies.

**Acknowledgments.** This work is jointly supported by the National Basic Research Program of China under Grant No 2012CB825601, the Knowledge Innovation Program of the Chinese Academy of Sciences (KZZD-EW-01-4), the National Natural Science Foundation of China (41231068, 41174150, 41274192, 41131065, 41121003 and 41274173), and the Specialized Research Fund for State Key Laboratories.

## References

- Burlaga, L. F., Plunkett, S. P. & St. Cyr, O. C. 2002 J. Geophys. Res., 107(A10)  
 Lugaz, N., Manchester, W. B., IV and Gombosi, T. I. 2005 Astrophys. J., 634 (1), 651-662  
 Lugaz, N. and Roussev, I. I. 2011 J. Atmosph. Terrest. Phys., 73 (10), 1187-1200  
 Shen, C. L., Yuming Wang, Shui Wang et al. 2012 Nature Phys., 8, 923-928  
 Shen, F., Feng, X., Wang, Y., Wu, S. T., Song, W. B., Guo, J. P. & Zhou, Y. F. 2011 J. Geophys. Res., 116, A09103  
 Shen, F., Wu, S. T., Feng, X. & Wu, C.-C. 2012 J. Geophys. Res., 117, A11101  
 Wang, Y. M., Ye, P. Z. & Wang, S. 2003 J. Geophys. Res., 108(A10), 1370.  
 Wang, Y., J. Zhang & C. Shen 2009 J. Geophys. Res., 114, A10,104